Observation of a Near-Threshold Enhancement in the $e^+e^- \to \Lambda_c^+\Lambda_c^-$ Cross Section Using Initial-State Radiation

G. Pakhlova,[14] I. Adachi,[10] H. Aihara,[42] K. Arinstein,[1] V. Aulchenko,[1] T. Aushev,[19,14] A. M. Bakich,[39] V. Balagura,[14] I. Bedny,[1] V. Bhardwaj,[34] U. Bitenc,[15] A. Bondar,[1] A. Bozek,[28] M. Bračko,[21,15] J. Brodzicka,[10] T. E. Browder,[9] P. Chang,[27] A. Chen,[25] B. G. Cheon,[8] C.-C. Chiang,[27] R. Chistov,[14] I.-S. Cho,[47] S.-K. Choi,[7] Y. Choi,[38] J. Dalseno,[10] M. Danilov,[14] M. Dash,[46] S. Eidelman,[1] N. Gabyshev,[1] H. Ha,[17] J. Haba,[10] K. Hayasaka,[23] M. Hazumi,[10] D. Heffernan,[33] Y. Hoshi,[41] W.-S. Hou,[27] Y. B. Hsiung,[27] H. J. Hyun,[18] T. Iijima,[23] K. Inami,[23] A. Ishikawa,[35] H. Ishino,[43,*] R. Itoh,[10] M. Iwasaki,[42] Y. Iwasaki,[10] D. H. Kah,[18] J. H. Kang,[47] N. Katayama,[10] H. Kawai,[2] T. Kawasaki,[30] H. Kichimi,[10] H. J. Kim,[18] H. O. Kim,[18] S. K. Kim,[37] Y. I. Kim,[18] Y. J. Kim,[6] K. Kinoshita,[3,15] P. Križan,[20,15] P. Krokovny,[10] R. Kumar,[34] A. Kuzmin,[1] Y.-J. Kwon,[47] S.-H. Kyeong,[47] J. S. Lange,[5] J. S. Lee,[38] S. E. Lee,[37] T. Lesiak,[28,4] J. Li,[9] A. Limosani,[22] C. Liu,[36] D. Liventsev,[14] F. Mandl,[12] A. Matyja,[28] K. Miyabayashi,[24] H. Miyata,[30] Y. Miyazaki,[23] R. Mizuk,[14] T. Mori,[23] E. Nakano,[32] M. Nakao,[10] Z. Natkaniec,[28] S. Nishida,[10] O. Nitoh,[45] S. Noguchi,[24] S. Ogawa,[40] T. Ohshima,[23] S. Okuno,[16] S. L. Olsen,[9,11] H. Ozaki,[10] P. Pakhlov,[14] H. Palka,[28] C. W. Park,[38] H. Park,[18] H. K. Park,[18] L. S. Peak,[39] L. E. Piilonen,[46] A. Poluektov,[1] H. Sahoo,[9] Y. Sakai,[10] O. Schneider,[19] K. Senyo,[23] M. Shapkin,[13] C. P. Shen,[9] J.-G. Shiu,[27] B. Shwartz,[1] J. B. Singh,[34] A. Sokolov,[13] S. Stanič,[31] M. Starič,[15] T. Sumiyoshi,[44] M. Tanaka,[10] G. N. Taylor,[22] Y. Teramoto,[32] I. Tikhomirov,[14] S. Uehara,[10] T. Uglov,[14] Y. Unno,[8] S. Uno,[10] P. Urquijo,[22] Y. Usov,[1] G. Varner,[9] C. H. Wang,[26] M.-Z. Wang,[27] P. Wang,[48] X. L. Wang,[11] Y. Watanabe,[16] R. Wedd,[22] E. Won,[17] B. D. Yabsley,[39] Y. Yamashita,[29] M. Yamauchi,[10] C. Z. Yuan,[11] C. C. Zhang,[11] Z. P. Zhang,[36] V. Zhilich,[1] V. Zhulanov,[1] T. Zivko,[15] A. Zupanc,[15] and O. Zyukova[1]

(The Belle Collaboration)

[1]*Budker Institute of Nuclear Physics, Novosibirsk*
[2]*Chiba University, Chiba*
[3]*University of Cincinnati, Cincinnati, Ohio 45221*
[4]*T. Kościuszko Cracow University of Technology, Krakow*
[5]*Justus-Liebig-Universität Gießen, Gießen*
[6]*The Graduate University for Advanced Studies, Hayama*
[7]*Gyeongsang National University, Chinju*
[8]*Hanyang University, Seoul*
[9]*University of Hawaii, Honolulu, Hawaii 96822*
[10]*High Energy Accelerator Research Organization (KEK), Tsukuba*
[11]*Institute of High Energy Physics, Chinese Academy of Sciences, Beijing*
[12]*Institute of High Energy Physics, Vienna*
[13]*Institute of High Energy Physics, Protvino*
[14]*Institute for Theoretical and Experimental Physics, Moscow*
[15]*J. Stefan Institute, Ljubljana*
[16]*Kanagawa University, Yokohama*
[17]*Korea University, Seoul*
[18]*Kyungpook National University, Taegu*
[19]*École Polytechnique Fédérale de Lausanne (EPFL), Lausanne*
[20]*Faculty of Mathematics and Physics, University of Ljubljana, Ljubljana*
[21]*University of Maribor, Maribor*
[22]*University of Melbourne, School of Physics, Victoria 3010*
[23]*Nagoya University, Nagoya*
[24]*Nara Women's University, Nara*
[25]*National Central University, Chung-li*
[26]*National United University, Miao Li*
[27]*Department of Physics, National Taiwan University, Taipei*
[28]*H. Niewodniczanski Institute of Nuclear Physics, Krakow*
[29]*Nippon Dental University, Niigata*
[30]*Niigata University, Niigata*
[31]*University of Nova Gorica, Nova Gorica*
[32]*Osaka City University, Osaka*

[33]Osaka University, Osaka
[34]Panjab University, Chandigarh
[35]Saga University, Saga
[36]University of Science and Technology of China, Hefei
[37]Seoul National University, Seoul
[38]Sungkyunkwan University, Suwon
[39]University of Sydney, Sydney, New South Wales
[40]Toho University, Funabashi
[41]Tohoku Gakuin University, Tagajo
[42]Department of Physics, University of Tokyo, Tokyo
[43]Tokyo Institute of Technology, Tokyo
[44]Tokyo Metropolitan University, Tokyo
[45]Tokyo University of Agriculture and Technology, Tokyo
[46]Virginia Polytechnic Institute and State University, Blacksburg, Virginia 24061
[47]Yonsei University, Seoul
[48]Institute of High Energy Physics, Chinese Academy of Sciences, Beijing
(Received 28 July 2008; published 24 October 2008)

We report a measurement of the exclusive $e^+e^- \to \Lambda_c^+\Lambda_c^-$ cross section as a function of center-of-mass energy near the $\Lambda_c^+\Lambda_c^-$ threshold. A clear peak with a significance of 8.2σ is observed in the $\Lambda_c^+\Lambda_c^-$ invariant mass distribution just above threshold. With an assumption of a resonance origin for the observed peak, a mass and width of $M = [4634^{+8}_{-7}(\mathrm{stat})^{+5}_{-8}(\mathrm{syst})]\ \mathrm{MeV}/c^2$ and $\Gamma_{\mathrm{tot}} = [92^{+40}_{-24}(\mathrm{stat})^{+10}_{-21}(\mathrm{syst})]$ MeV are determined. The analysis is based on a study of events with initial-state-radiation photons in a data sample collected with the Belle detector at the $\Upsilon(4S)$ resonance and nearby continuum with an integrated luminosity of 695 fb^{-1} at the KEKB asymmetric-energy e^+e^- collider.

DOI: 10.1103/PhysRevLett.101.172001 PACS numbers: 13.66.Bc, 13.87.Fh, 14.40.Gx

The discovery of many unexpected charmoniumlike states has stimulated renewed interest in charmonium physics. Among these new states, the $Y(4260)$ [1,2], $Y(4360)$, and $Y(4660)$ [3,4] have quantum numbers $J^{PC} = 1^{--}$ and are produced via e^+e^- annihilation. Surprisingly, no evidence for open-charm production associated with these new states has been observed. Moreover, the parameters of the conventional charmonium 1^{--} states obtained from fits to the inclusive cross section [5] remain poorly understood theoretically [6]. Measurements of exclusive cross sections for charmed meson and baryon pairs in the 4 to 5 GeV energy range are needed to help clarify the situation.

Initial-state radiation (ISR) provides a powerful tool for measuring exclusive e^+e^- cross sections at $\sqrt{s}$ smaller than the initial e^+e^- center-of-mass (c.m.) energy ($E_{\mathrm{c.m.}}$) at B-factories. ISR allows one to obtain cross sections over a broad energy range, while the high luminosity of the B-factories compensates for the suppression associated with the emission of a hard photon. The first measurements of the exclusive cross sections for $e^+e^- \to D^{(*)\pm}D^{*\mp}$ for $\sqrt{s}$ near the $D^{(*)\pm}D^{*\mp}$ thresholds were performed by Belle [7]. Subsequently, *BABAR* [8] and Belle [9] presented exclusive $e^+e^- \to D\bar{D}$ production measurements via ISR. Recently, Belle [10] reported a measurement of the exclusive cross section for $e^+e^- \to D^0D^-\pi^+$ [11] and the first observation of $\psi(4415) \to D\bar{D}_2^*(2460)$ decay. These measured final states almost saturate the total cross section for hadron production in e^+e^- annihilation in the $\sqrt{s}$ region up to $\sim$4.3 GeV. The thresholds for charm baryon-antibaryon pair production lie in the energy range above 4.5 GeV, where experimental data are limited [12] or unavailable.

In this Letter, we report the first measurement of the exclusive cross section for the process $e^+e^- \to \Lambda_c^+\Lambda_c^-$ via ISR and the first observation of a resonantlike structure at threshold. The data sample corresponds to an integrated luminosity of 695 fb^{-1} collected with the Belle detector [13] at the $\Upsilon(4S)$ resonance and nearby continuum at the KEKB asymmetric-energy e^+e^- collider [14].

The selection of $e^+e^- \to \Lambda_c^+\Lambda_c^-\gamma_{\mathrm{isr}}$ signal events using full reconstruction of both the Λ_c^+ and Λ_c^- baryons suffers from the low Λ_c reconstruction efficiency and small branching fractions for decays to accessible final states. Therefore, in order to achieve higher efficiency, we require full reconstruction of only one of the Λ_c baryons and the γ_{ISR} photon. In this case, the spectrum of masses recoiling against the $\Lambda_c^+\gamma_{\mathrm{ISR}}$ system,

$$M_{\mathrm{rec}}(\Lambda_c^+\gamma_{\mathrm{ISR}}) = \sqrt{(E_{\mathrm{c.m.}} - E^*_{\Lambda_c^+\gamma_{\mathrm{ISR}}})^2 - p^{*2}_{\Lambda_c^+\gamma_{\mathrm{ISR}}}}, \quad (1)$$

peaks at the Λ_c^- mass. Here, $E^*_{\Lambda_c^+\gamma_{\mathrm{ISR}}}$ and $p^*_{\Lambda_c^+\gamma_{\mathrm{ISR}}}$ are the center-of-mass energy and momentum, respectively, of the $\Lambda_c^+\gamma_{\mathrm{ISR}}$ combination. The $M_{\mathrm{rec}}(\Lambda_c^+\gamma_{\mathrm{ISR}})$ peak is broad [$\sigma_{M_{\mathrm{rec}}} \sim 250\ \mathrm{MeV}/c^2$ according to a Monte Carlo (MC) simulation] and asymmetric due to the photon energy resolution and higher-order ISR processes (i.e., more than one γ_{ISR} in the event). This makes the distinction between $\Lambda_c^+\Lambda_c^-$, $\Lambda_c^+\Lambda_c^-\pi^0$, and $\Lambda_c^+\Lambda_c^-\pi\pi$ final states difficult.

For the measurement of the exclusive cross section for $e^+e^- \to \Lambda_c^+\Lambda_c^-$, we determine the mass recoiling against the $\gamma_{\rm ISR}$ photon $[M_{\rm rec}(\gamma_{\rm ISR})]$, which is equivalent to $M(\Lambda_c^+\Lambda_c^-)$ in the absence of higher-order QED processes. To improve the $M_{\rm rec}(\gamma_{\rm ISR})$ resolution (expected to be $\sim$100 MeV/c^2), we apply a refit that constrains $M_{\rm rec}(\Lambda_c^+\gamma_{\rm ISR})$ to the nominal Λ_c^- mass. In this way, we use the well measured properties of the fully reconstructed Λ_c^+ to correct the poorly measured energy of the $\gamma_{\rm ISR}$. As a result, the $M_{\Lambda_c^+\Lambda_c^-}$ resolution is improved substantially; it varies from $\sim$3 MeV/c^2 just above threshold to $\sim$8 MeV/c^2 at $M_{\Lambda_c^+\Lambda_c^-} \sim 5.4$ GeV/c^2.

All charged tracks are required to originate from the vicinity of the interaction point (IP); we impose the requirements $dr < 1$ cm and $|dz| < 4$ cm, where dr and $|dz|$ are the impact parameters perpendicular to and along the beam direction with respect to the IP. Particle identification requirements are based on dE/dx, aerogel Cherenkov and time-of-flight counter information [15]. Protons and charged kaons have typical misidentification probabilities less than 0.1. No identification requirements are applied for pion candidates. K_S^0 (Λ) candidates are reconstructed from $\pi^+\pi^-$ ($p\pi^-$) pairs with an invariant mass within 10 MeV/c^2 ($\sim 3\sigma$) of the K_S^0 (Λ) mass. The distance between the two pion (proton and pion) tracks at the K_S^0 (Λ) vertex must be less than 1 cm, the transverse flight distance from the interaction point is required to be greater than 0.1 cm, and the angle between the K_S^0 (Λ) momentum direction and the flight direction in the x-y plane should be less than 0.01(0.005) rad. Photons are reconstructed in the electromagnetic calorimeter as showers with energies greater than 50 MeV that are not associated with charged tracks. ISR photon candidates are required to have energies greater than 3.5 GeV. Candidate π^0 mesons are formed from pairs of photons. If the mass of a $\gamma\gamma$ pair lies within 15 MeV/c^2 ($\sim 3\sigma$) of the π^0 mass, the pair is fit with a π^0 mass constraint and considered as a π^0 candidate.

Λ_c^+ candidates are reconstructed using three decay modes: pK_S^0, $pK^-\pi^+$, and $\Lambda\pi^+$. The mass distribution of Λ_c^+ candidates from $\Lambda_c^+\gamma_{\rm ISR}$ combinations is shown in Fig. 1(a). To suppress combinatorial background, we require the presence of at least one $\bar{p}$ in the event from the decay of the unreconstructed Λ_c^- ($\bar{p}$ tag). As a result, the combinatorial background is suppressed by a factor of $\sim$10 at the expense of about a 40% reduction in signal according to the MC simulation [see Fig. 1(b)].

A ± 10 MeV/c^2 mass window is used for all Λ_c^+ candidate decay modes ($\sim 2.5\sigma$ in each case). To improve the momentum resolution of Λ_c^+ candidates, final tracks are fitted to a common vertex with a mass constraint to the Λ_c^+ mass. Only one $\Lambda_c^+\gamma_{\rm ISR}$ combination per event is accepted; in the case of multiple combinations, which occur in 5% of the candidate events, the combination with the best χ^2 for the Λ_c^+ mass fit is selected. Λ_c^+ mass sidebands selected for the background study are 4 times as large as the signal region. To avoid signal over-subtraction, the sidebands are shifted by 20 MeV/c^2 from the signal region. The sidebands are divided into windows of the same width as that for the signal. The Λ_c^+ candidates from these sidebands are refitted to the central mass value of each window, and a single candidate in each window per event is selected.

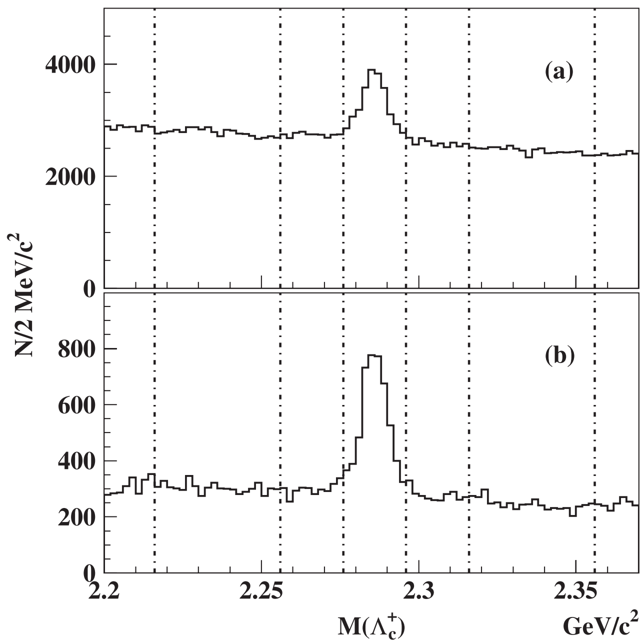

FIG. 1. The mass distribution of Λ_c^+ from $\Lambda_c^+\gamma_{\rm ISR}$ combinations: (a) without a $\bar{p}$ tag; (b) with a $\bar{p}$ tag. The Λ_c^+ signal and background regions are indicated by vertical lines.

The distribution of $M_{\rm rec}(\Lambda_c^+\gamma_{\rm ISR})$ with a $\bar{p}$ tag is shown in Fig. 2. The excess around the Λ_c^- mass includes the $e^+e^- \to \Lambda_c^+\Lambda_c^-\gamma_{\rm isr}$ signal as well as possible reflections from the $e^+e^- \to \Lambda_c^+\Lambda_c^-\pi^0\gamma_{\rm isr}$ and $e^+e^- \to \Lambda_c^+\Lambda_c^-\pi\pi\gamma_{\rm isr}$ processes with an additional π^0 or $\pi\pi$, respectively, in the final state. The process $e^+e^- \to \Lambda_c^+\Lambda_c^-\pi^0\gamma_{\rm isr}$, which could proceed via $e^+e^- \to \Lambda_c^+\Sigma_c^-\gamma_{\rm isr}$, violates isospin and is expected to be strongly suppressed. The process $e^+e^- \to \Lambda_c^+\Lambda_c^-\pi\pi\gamma_{\rm isr}$ is allowed and is expected to proceed via $\Lambda_c^+\Lambda_c^-(2595)$, $\Lambda_c^+\Lambda_c^-(2625)$, $\Lambda_c^+\Lambda_c^-(2765)$, and $\Lambda_c^+\Lambda_c^-(2880)$ final states. Each final state would produce a broad peak in the $M_{\rm rec}(\Lambda_c^+\gamma_{\rm ISR})$ distribution around the corresponding mass value (i.e., $m_{\Sigma_c^-}$, $m_{\Lambda^-(2595)}$, $m_{\Lambda^-(2625)}$, $m_{\Lambda^-(2765)}$, and $m_{\Lambda^-(2880)}$). Because of the poor $M_{\rm rec}(\Lambda_c^+\gamma_{\rm ISR})$ resolution, these peaks overlap and appear as a shoulder for masses above $\sim$2.5 GeV/c^2.

To estimate the contribution from the reflections and to optimize the signal region requirement, we fit the $M_{\rm rec}(\Lambda_c^+\gamma_{\rm ISR})$ distribution with the sum of a signal plus a combinatorial and reflection background with normalizations left as free parameters. To describe the combinatorial

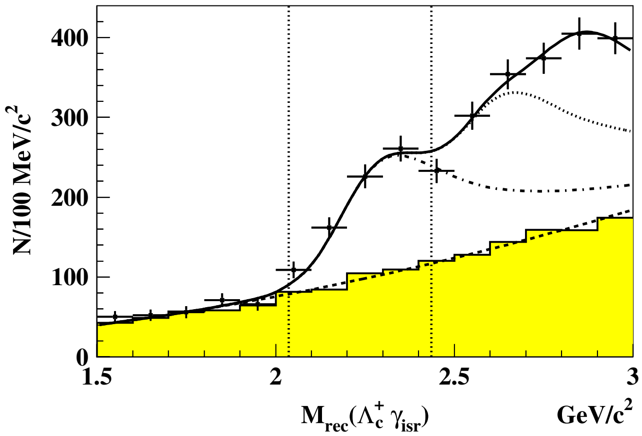

FIG. 2 (color online). The $M_{\rm rec}(\Lambda_c^+\gamma_{\rm ISR})$ distribution with a $\bar{p}$ tag. The solid curve represents the result of the fit described in the text. The combinatorial background parameterization is shown by the dashed curve. The dashed-dotted curve represents a contribution of the $\Lambda_c^+\Lambda_c^-$ final state while the dotted curve is that of the $\Lambda_c^+\Lambda_c^-(2595)$ and the $\Lambda_c^+\Lambda_c^-(2625)$ final states. The difference between the solid and dotted lines corresponds to the contribution of the $\Lambda_c^+\Lambda_c^-(2765)$ and the $\Lambda_c^+\Lambda_c^-(2880)$ final states. The histogram shows the normalized $M_{\Lambda_c^+}$ sidebands contributions. The selected signal window is indicated by the vertical lines.

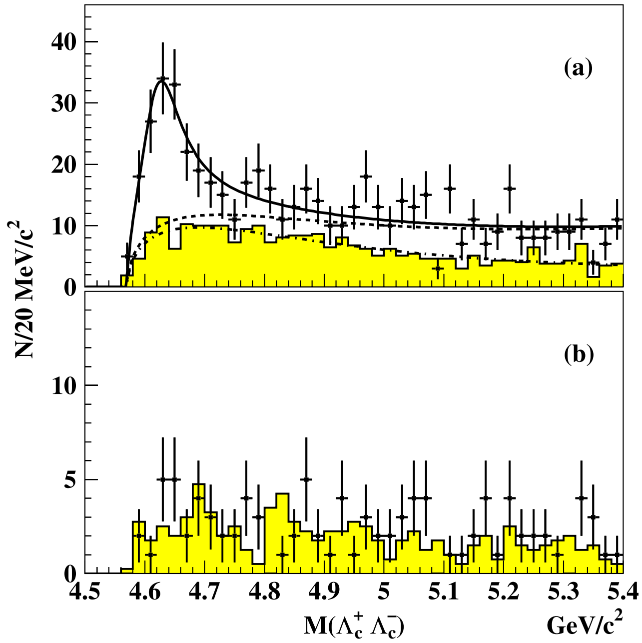

FIG. 3 (color online). The $M_{\Lambda_c^+\Lambda_c^-}$ spectrum for the signal region: (a) with $\bar{p}$ tag. The solid curve represents the result of the fit described in the text. The threshold function is shown by the dashed curve. The combinatorial background parameterization is shown by the dashed-dotted curve; (b) with proton (wrong-sign) tag. Histograms show the normalized contributions from Λ_c^+ sidebands.

background, we use Λ_c^+ sideband data parameterized by a second-order polynomial. We perform a simultaneous likelihood fit to the $M_{\rm rec}(\Lambda_c^+\gamma_{\rm ISR})$ signal and sideband spectra. The signal and reflection shapes of the $\Lambda_c^+\Sigma_c^-$, $\Lambda_c^+\Lambda_c^-(2595)$, $\Lambda_c^+\Lambda_c^-(2625)$, $\Lambda_c^+\Lambda_c^-(2765)$, $\Lambda_c^+\Lambda_c^-(2880)$ final states are fixed from the MC simulation. All reflection normalizations are floated separately in the fit. The goodness of the fit is found to be $\chi^2/\text{n.d.f} = 18.8/22$. We define an asymmetric requirement on $M_{\rm rec}(\Lambda_c^+\gamma_{\rm ISR})$ of $-250\ \text{MeV}/c^2 < m_{\Lambda_c^-} < 150\ \text{MeV}/c^2$ to suppress the dominant part of the reflection background, as shown in Fig. 2. We find 386 ± 27 signal events in this signal region. The contribution of the process $e^+e^- \to \Lambda_c^+\Lambda_c^-\pi^0\gamma_{\rm isr}$ in the signal region is estimated to be less than 18 events at the 90% C.L. while that from the $e^+e^- \to \Lambda_c^+\Lambda_c^-\pi\pi\gamma_{\rm isr}$ process is estimated to be 7.3 ± 1.7 events. In the following study, the possible contribution of these backgrounds is included in the systematic error.

The contribution from $e^+e^- \to \Lambda_c^+\Lambda_c^-\pi^0$, where an energetic π^0 is misidentified as a single $\gamma_{\rm ISR}$, is found to be negligibly small. This is determined from a study of $e^+e^- \to \Lambda_c^+\Lambda_c^-\pi^0$ events using a similar reconstruction technique, but with an energetic π^0 replacing the $\gamma_{\rm ISR}$.

The $M_{\Lambda_c^+\Lambda_c^-}$ spectrum for events in the signal region is shown in Fig. 3(a). A clear peak is evident near the $\Lambda_c^+\Lambda_c^-$ threshold. We perform a simultaneous likelihood fit to the $M_{\Lambda_c^+\Lambda_c^-}$ distributions for the Λ_c^+ signal and sideband regions to fix the combinatorial background shapes. The combinatorial background is parameterized by $p_1\sqrt{M - M_{\rm thr}}e^{-(p_2M+p_3M^2)}$, where p_1, p_2, and p_3 are free parameters. The signal function is a sum of a relativistic s-wave Breit-Wigner (RBW) function [16] and a threshold function $\sqrt{M - M_{\rm thr}}$ with a floating normalization to take into account a possible nonresonant contribution. Finally, the sum of the signal resonance and nonresonant functions is multiplied by an efficiency function that has a linear dependence on $M_{\Lambda_c^+\Lambda_c^-}$, and the differential ISR luminosity, described in Ref. [7]. The fit, shown as a solid curve in Fig. 3(a), attributes 142^{+32}_{-28} events to the RBW signal. The obtained peak mass is $M = [4634^{+8}_{-7}(\text{stat})^{+5}_{-8}(\text{syst})]\ \text{MeV}/c^2$ and the total width is $\Gamma_{\rm tot} = [92^{+40}_{-24}(\text{stat})^{+10}_{-21}(\text{syst})]$ MeV. The fit gives $\chi^2/\text{n.d.f} = 104/77$. Here, the systematic uncertainties are obtained by varying the fit range, histogram bin size, efficiency function, parameterization of the background function, and the nonresonant parametrization. The systematic error associated with the possible interference between the resonance and nonresonant contributions is estimated from the fit with a coherent sum of the RBW and nonresonant amplitudes, which has the quality $\chi^2/\text{n.d.f} = 103/76$ and yields a smaller mass ($4626\ \text{MeV}/c^2$) and total width (77 MeV). A statistical significance for the signal of 8.8σ is determined from the quantity $-2\ln(\mathcal{L}_0/\mathcal{L}_{\rm max})$, where $\mathcal{L}_{\rm max}$ is the maximum likelihood returned by the fit, and $\mathcal{L}_0$ is the likelihood with the amplitude of the Breit-Wigner function set to zero, taking the reduction in the number of degrees of freedom into account. The significance including systematics is 8.2σ. We use $X(4630)$ to denote the observed structure.

As a cross check, we present in Fig. 3(b) the $M_{\Lambda_c^+\Lambda_c^-}$ spectrum for the signal region for wrong-sign tags, i.e., requiring a presence of a proton in the event in addition to the $\Lambda_c^+\gamma_{\rm ISR}$ combination. The $M_{\Lambda_c^+\Lambda_c^-}$ distribution from the signal Λ_c^+ window is in good agreement with the normalized contributions from the Λ_c^+ sidebands.

The $e^+e^-\to\Lambda_c^+\Lambda_c^-$ cross section is extracted from the background-subtracted $\Lambda_c^+\Lambda_c^-$ mass distribution following the procedure described in Ref. [7], taking into account the differential ISR luminosity and the efficiency function. The resulting $e^+e^-\to\Lambda_c^+\Lambda_c^-$ exclusive cross section is shown in Fig. 4 with statistical uncertainties only. Since the bin width is much larger than resolution, no correction for resolution is applied.

The peak cross section for the $e^+e^-\to\Lambda_c^+\Lambda_c^-$ process at $E_{\rm c.m.}=m_{X(4630)}$ is calculated from the amplitude of the RBW function in the fit to be $\sigma(e^+e^-\to X(4630))\times\mathcal{B}(X(4630)\to\Lambda_c^+\Lambda_c^-)=[0.47^{+0.11}_{-0.10}({\rm stat})^{+0.05}_{-0.08}({\rm syst})\pm 0.19({\rm syst})]$ nb. Here the first systematic uncertainty is obtained by varying the fit range, histogram bin, parameterization of the background function, efficiency and the possible interference between the resonance and nonresonant contributions. The second one comes from the uncertainties in $\mathcal{B}(\Lambda_c^+\to pK^-\pi^+)=(5.0\pm1.3)\times10^{-2}$ and $\mathcal{B}(\Lambda_c^-\to\bar{p}X)=(50\pm16)\times10^{-2}$ [16]. Using $\sigma(e^+e^-\to X(4630))=12\pi/m^2_{X(4630)}\times(\Gamma_{ee}/\Gamma_{\rm tot})$ and the $X(4630)$ mass value obtained from the fit we calculate $\Gamma_{ee}/\Gamma_{\rm tot}\times\mathcal{B}(X(4630)\to\Lambda_c^+\Lambda_c^-)=[0.68^{+0.16}_{-0.15}({\rm stat})^{+0.07}_{-0.11}({\rm syst})\pm0.28({\rm syst})]\times10^{-6}$.

The various contributions to the systematic errors for the $\sigma(e^+e^-\to\Lambda_c^+\Lambda_c^-)$ measurements are summarized in Table I. The systematic errors associated with the combinatorial background subtraction are estimated to be 3% due to an uncertainty in the scaling factors for the sideband subtractions. It is estimated using fits to the $M_{\Lambda_c^+}$ distribution with different signal and background parameterizations. Reflections from the $e^+e^-\to\Lambda_c^+\Lambda_c^-\pi^0\gamma_{\rm isr}$ and $e^+e^-\to\Lambda_c^+\Lambda_c^-\pi\pi\gamma_{\rm isr}$ processes are estimated conservatively to be smaller than 6% of the signal. The uncertainty due to a possible $e^+e^-\to\Lambda_c^+\Lambda_c^-\pi^0$ contribution is found to be 1%. The systematic error ascribed to the cross section calculation includes a 1.5% error on the differential luminosity and 2% error due to the MC statistics. Another source of systematic error comes from uncertainties in track and photon reconstruction efficiencies (1% per track and 1.5% per photon). Another contribution comes from the uncertainty in the kaon and proton identification efficiency. The systematic uncertainty due to the unknown helicity angle distribution for the $\Lambda_c^+\Lambda_c^-$ final state is included. For the efficiency calculation, we use a flat helicity distribution and consider the extreme cases $dN/d\cos\theta\sim 1+\cos^2\theta$ and $\sim\sin^2\theta$ for the efficiency uncertainty.

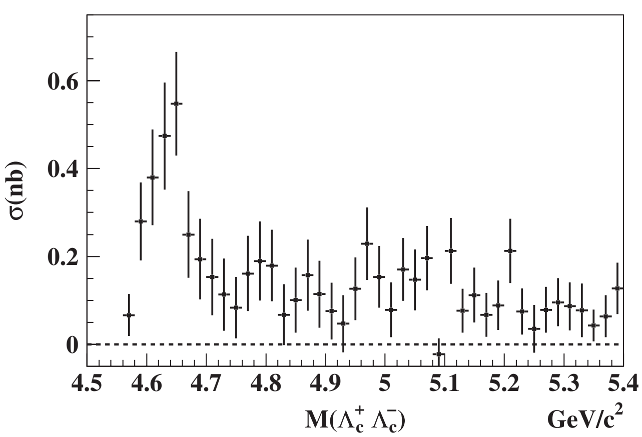

FIG. 4. The cross section for the exclusive process $e^+e^-\to\Lambda_c^+\Lambda_c^-$.

In summary, we report the first measurements of the $e^+e^-\to\Lambda_c^+\Lambda_c^-$ exclusive cross section over the center-of-mass energy range from the threshold to 5.4 GeV with initial-state radiation. We observe a significant near-threshold enhancement in the studied cross section. The nature of this enhancement remains unclear. In many processes including three-body B meson baryonic decays, mass peaks are observed near-threshold [17]. However, the cross section for $e^+e^-\to\Lambda\bar{\Lambda}$ measured via ISR by *BABAR* [18] has a different pattern: it increases sharply at threshold and then decreases gradually without any peaklike structure. Assuming the observed peak to be a resonance, its mass and width are found to be $M=[4634^{+8}_{-7}({\rm stat})^{+5}_{-8}({\rm syst})]$ MeV$/c^2$ and $\Gamma_{\rm tot}=[92^{+40}_{-24}({\rm stat})^{+10}_{-21}({\rm syst})]$ MeV, respectively. These values are consistent within errors with the mass and width of a new 1^{--} charmoniumlike state, the $Y(4660)$, that was found in $\psi(2S)\pi\pi$ decays via ISR [4]. Finally, we cannot exclude the possibility that the observed enhancement is the 5^3S_1 charmonium state that is predicted around the observed mass [19].

We thank the KEKB group for excellent operation of the accelerator, the KEK cryogenics group for efficient solenoid operations, and the KEK computer group and the NII

TABLE I. Contributions to the systematic error on the cross sections, [%].

Source	$\Lambda_c^+\Lambda_c^-$
Background subtraction	±7
Cross section calculation	±3
Reconstruction	±5
Identification	±3
Angular distributions	±4
Total	±10
$\mathcal{B}(\Lambda_c^+)$	±26
$\mathcal{B}(\Lambda_c^-\to\bar{p}X)$	±32

for valuable computing and SINET3 network support. We acknowledge support from MEXT and JSPS (Japan); ARC and DEST (Australia); NSFC (China); DST (India); MOEHRD, KOSEF and KRF (Korea); KBN (Poland); MES and RFAAE (Russia); ARRS (Slovenia); SNSF (Switzerland); NSC and MOE (Taiwan); and DOE (USA).

*Now at Okayama University, Okayama

[1] B. Aubert *et al.* (*BABAR* Collab.), Phys. Rev. Lett. **95**, 142001 (2005).
[2] C. Z. Yuan *et al.* (Belle Collab.), Phys. Rev. Lett. **99**, 182004 (2007).
[3] B. Aubert *et al.* (*BABAR* Collab.), Phys. Rev. Lett. **98**, 212001 (2007).
[4] X. L. Wang *et al.* (Belle Collab.), Phys. Rev. Lett. **99**, 142002 (2007).
[5] M. Ablikim *et al.* (BES Collab.), Phys. Lett. B **660**, 315 (2008).
[6] T. Barnes, S. Godfrey, and E. S. Swanson, Phys. Rev. D **72**, 054026 (2005).
[7] G. Pakhlova *et al.* (Belle Collab.), Phys. Rev. Lett. **98**, 092001 (2007).
[8] B. Aubert *et al.* (*BABAR* Collab.), Phys. Rev. D **76**, 111105 (2007).
[9] G. Pakhlova *et al.* (Belle Collab.), Phys. Rev. D **77**, 011103 (2008).
[10] G. Pakhlova *et al.* (Belle Collab.), Phys. Rev. Lett. **100**, 062001 (2008).
[11] Charge-conjugate modes are included throughout this Letter.
[12] G. S. Abrams *et al.*, Phys. Rev. Lett. **44**, 10 (1980).
[13] A. Abashian *et al.* (Belle Collab.), Nucl. Instrum. Methods Phys. Res., Sect. A **479**, 117 (2002).
[14] S. Kurokawa and E. Kikutani, Nucl. Instrum. Methods Phys. Res., Sect. A **499**, 1 (2003); and other papers included in this volume.
[15] E. Nakano, Nucl. Instrum. Methods Phys. Res., Sect. A **494**, 402 (2002).
[16] W.-M. Yao *et al.* (Particle Data Group), J. Phys. G **33**, 1 (2006).
[17] For example: S. Anderson *et al.* (CLEO Collab.), Phys. Rev. Lett. **86**, 2732 (2001); K. Abe *et al.* (Belle Collab.), *ibid.* **89**, 151802 (2002); **88**, 181803 (2002); M. Z. Wang *et al.* (Belle Collab.), *ibid.* **90**, 201802 (2003); N. Gabyshev *et al.* (Belle Collab.), *ibid.* **97**, 242001 (2006); J. L. Rosner, Phys. Rev. D **68**, 014004 (2003).
[18] B. Aubert *et al.* (*BABAR* Collab.), Phys. Rev. D **76**, 092006 (2007).
[19] A. M. Badalian, B. L. G. Bakker, and I. V. Danilkin, arXiv:0805.2291.